Japanese Journal of Applied Physics **54**, 02BB02 (2015) **REGULAR PAPER**
http://dx.doi.org/10.7567/JJAP.54.02BB02

GaInN-based light emitting diodes embedded with wire grid polarizers

Jaehee Cho[1*], David S. Meyaard[2], Ming Ma[2], and E. Fred Schubert[2]

[1]*School of Semiconductor and Chemical Engineering, Semiconductor Physics Research Center, Chonbuk National University, Jeonju 561-756, Korea*
[2]*Future Chips Constellation, Department of Electrical, Computer, and Systems Engineering, Rensselaer Polytechnic Institute, Troy, NY 12180, U.S.A.*
E-mail: jcho@chonbuk.ac.kr

Received June 2, 2014; accepted October 11, 2014; published online December 22, 2014

The use of liquid crystal displays (LCDs) has become prevalent in our modern, technology driven society. We demonstrate a linearly polarized GaInN light-emitting diode (LED) embedded with a wire-grid polarizer (WGP). A derivation of rigorous coupled-wave analysis is given; starting from Maxwell's equations and finishing by matching the boundary conditions in the grating and other regions of interest. Simulated results are shown for various grating parameters, including different metals used for the grating and the metal-line dimensions. An LED fabrication process is developed for demonstrating WGP-LEDs. A clear polarization preference for the light coming out of the WGP-LED is experimentally demonstrated with a polarization ratio over 0.90, which is in good agreement with simulation results. © 2015 The Japan Society of Applied Physics

1. Introduction

Liquid crystal displays (LCDs) are main components of many popular consumer electronic devices, including cellular telephones and flat panel televisions.[1–3] The largest market for LCDs is for their use in televisions. There were approximately 596 million households worldwide that paid for a television subscription in 2009.[4] Current LCD TVs consume about 100 to 400 W during operation, depending on the size and technology. This globally represents a significant use of energy, so it is desirable to increase the efficiency of LCDs as much as possible. In typical LCD systems, transparent electrical contacts are made with indium tin oxide (ITO) which allows a voltage to be applied across the liquid crystals.[5,6] If no voltage is applied, the electric field from light incident on these liquid crystals will rotate 90° with the orientation of the crystals. If some voltage is applied to the crystals, however, they untwist proportionally to the amount of voltage that is applied to them. When polarizing filters are placed perpendicularly before and after the liquid crystals, the amount of light allowed through can be switched from no light to full transmission. This means that for light to be useful in an LCD, first the light must be polarized. In other words, the light that enters an LCD must be polarized in order for the system to work. Currently absorptive polarizers are used in commercial LCDs which result in about 50% loss of light.[5] Apart from the color filters, this is the largest loss of energy in an LCD system. If a polarized light source is used instead, the loss by absorptive polarizers will be minimized; thus the energy efficiency of the LCD system will be significantly improved.

Televisions branded as "LED-TV" still utilize LCD technology, but are backlit by light-emitting diodes (LEDs).[7–9] Over the past several years, the number of LED-TVs has increased in production and sales because they are much lighter and thinner than their predecessors.[2,10] Among these systems, there are edge- and direct-lit panels. Direct-lit systems involve many LEDs that are placed behind the LCD, allowing for high brightness and easy local dimming. If these LEDs were already polarized, instead of having to go through an initial polarizer, as mentioned earlier, an approximately 50% increase in energy efficiency could be achieved from the backlight unit (BLU).

Wire-grid polarizers (WGPs) are well-known optical components, in the past primarily used in the infrared spectrum, but now available for a broader range including visible light.[11,12] WGPs rely on an array of conductive metal lines and their interaction with the electric field component of the incident light. The general concept is as follows: incident light with an electric field component parallel to the wire induces movement of the free electrons in the wire. These electrons then re-radiate, perfectly cancelling out the transmitted beam and reflecting all of the energy. If the light, however, has a component perpendicular to the array of wires, then the light is transmitted, since the dimension of each line is small enough that no significant movement of electrons can occur. Here we define transverse electric (TE) mode light as light whose electric field component oscillates perpendicular to the plane of incidence. Transverse magnetic (TM) mode light is when then magnetic field component oscillates perpendicular to the plane of incidence. For WGP to function properly, the size of the grating must be much less than the wavelength of incident light. Up until recently, this meant that the use of WGPs was limited to far infrared or longer wavelength. In recent years, however, several nano-size patterning techniques have been developed that allow for fabrication on the scale necessary for visible light. These techniques include nano-imprint lithography, laser interferometry, and electron-beam lithography.[13–15]

There have been many publications regarding the inherent advantages of GaN as a material system for polarized LEDs, both on LEDs grown on a non-polar plane[16–18] and on LEDs utilizing the light emitted out of the side wall of *c*-plane LEDs.[19] A polarization enhancing reflector was implemented to rotate the direction of the light anisotropically such that most of the light viewed from the top of the chip is polarized in one direction.[20] The polarization ratio for use in an LCD, however, was not high enough yet, because the light that escapes out of the top of the LED was not polarized when using this reflector. In order for polarized LEDs to be practical, it is necessary to find another complementary method for polarizing the light from the top. Embedding a WGP on top of an LED would allow for the desired polarization to be transmitted and for the undesired polarization to be reflected back, where it could either be scattered on the p-contact and have another chance to escape the polarizer. Although this design is conceptually simple, calculating the amount of light transmitted and reflected and fabricating the devices are less so. In this study, an unconventional method for a polarized light emission is

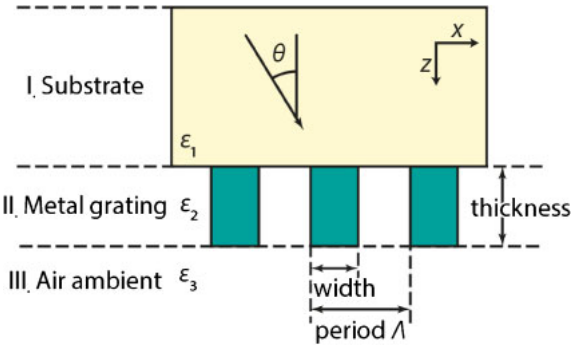

Fig. 1. (Color online) Schematic diagram of the simulated grating geometry, showing the *xz* coordinate system.

proposed, consisting of a WGP structure embedded on an LED chip. The theory and fabrication methods behind this WGP-LED are studied and discussed.

2. Theoretical calculation and computational simulation

Rigorous coupled wave analysis (RCWA) is applied to optimize the parameters of the grating.[21,22] In this method, Maxwell's equations are solved in three regions: the substrate, grating, and the ambient. Separate equations are considered and solved for the TE and TM mode light. The equations introduced in this paper are relevant to the TE mode; for the TM mode, a similar derivation can be performed. A complete derivation of equations and methods of solutions for both modes of light is found in the literature.[23,24] Figure 1 shows the geometry defined for this work, as well as the optimization parameters of interest. To simplify the theoretical calculations, the area of the polarizer is assumed to be infinitely large. For visible-light applications, the WGP will have several thousand periods per centimeter, so this assumption can be justified. In order to solve Maxwell's equations, the electric field in each of the three regions of interest should be first described. If we define the interface of the grating region to lie in the *y*-plane and consider the light to be a plane wave, any incident light can be generalized in terms of its *x* and *z* components, as shown in Fig. 1. We define the incident light in terms of its electric field components:

$$E_{\text{in}} = e^{-j(k_{x,0}x+k_{z,0}z)}, \tag{1}$$

where $k_{x,0}$ and $k_{z,0}$ is the 0th order wave vector in the *x*- and *z*-directions, respectively, and j is the imaginary number ($j^2 = -1$). When the incident wave reaches the grating, a set of waves will be reflected backwards. We can then express the electric field in region I as a sum of the incident and all reflected waves:

$$E_{\text{I}} = e^{-j(k_{x,0}x+k_{z,0}z)} + \sum_i R_i e^{-j(k_{x,i}x+k_{z,i,\text{I}}z)}, \tag{2}$$

where R_i is the amplitude of the ith order reflected wave, and $k_{z,i,\text{I}}$ refers to the ith order wave vector in the *z*-direction in region I.

The periodic grating, located in region II, is assumed to consist of two materials, in this case, metal and air. We can then express the electric field in the grating in terms of its complex field components. This is implemented in the equation:

$$E_{\text{II}} = \sum_i S_i(z) e^{-j(k_{x,i}x+k_{z,0}z)}, \tag{3}$$

where S_i is the normalized amplitude of the ith space harmonic field. For the grating region, we discretize parameters such as complex permittivity, $\varepsilon(x)$, by expressing them as a as sum of Fourier components:

$$\varepsilon(x) = \sum_p \varepsilon_p e^{jKpx}, \tag{4}$$

where ε_p is the pth Fourier component of the relative permittivity in the grating region, and Λ is the grating period with $K = 2\pi/\Lambda$.

In region III, there are no reflected waves, but simply the sum of waves transmitted through the grating:

$$E_{\text{III},y} = \sum_i T_i e^{-j(k_{x,i}x+k_{z,i,\text{II}}(z-d))}, \tag{5}$$

where T_i is the amplitude of the ith order transmitted wave and d is the thickness of the grating.

After defining the electric field in each region, we solve the Maxwell–Faraday equation in all areas of interest, resulting in a series of coupled differential equations. In order to discretize certain parameters, we do this in the derivation by solving the equation for each order of diffracted light, as well as expressing the complex permittivity inside of the grating in terms of its Fourier components. The transmitted and reflected waves can be solved by using the known electrostatic boundary conditions, such as continuous tangential E and H at the boundary interfaces ($z = 0$ and d). Here, we define the polarization ratio, PR, as

$$\text{PR} = \frac{|I_{\text{TE}} - I_{\text{TM}}|}{I_{\text{TE}} + I_{\text{TM}}}. \tag{6}$$

That is, unpolarized light ($I_{\text{TE}} = I_{\text{TM}}$) has a polarization ratio of zero and highly polarized light ($I_{\text{TM}} \gg I_{\text{TE}}$) has a polarization ratio of about one. Using this calculation method, we can compare the effect of all relevant parameters such as choice of metal, metal thickness, metal width, and grating period. It is desired to maximize not only transmitted light of the desired polarization, but also polarization ratio at the same time.

Before fabrication, a metal must be chosen for the grating. This must be based on the complex permittivity of each material. Intuitively, a highly conductive material would serve as the best metal for this purpose, such as gold, aluminum, or silver. These materials are compared to see which yields the best polarization ratio, as well as TM transmitted intensity. The wavelength of light used in this simulation is 460 nm, typical for a GaInN/GaN LED. As shown in Fig. 2, both silver and gold yield poor results compared to aluminum; the overlap of high TM transmitted intensity and high polarization ratio is not as strong as in the case of aluminum.

The other parameters that must be decided are the width of the metal lines, the period of the grating, and the thickness of the metal lines. All three parameters are adjusted in order to find an optimum point. As shown in Fig. 3, these simulations show that there is a clear tradeoff between the TM mode optical power transmitted and polarization ratio. In general,

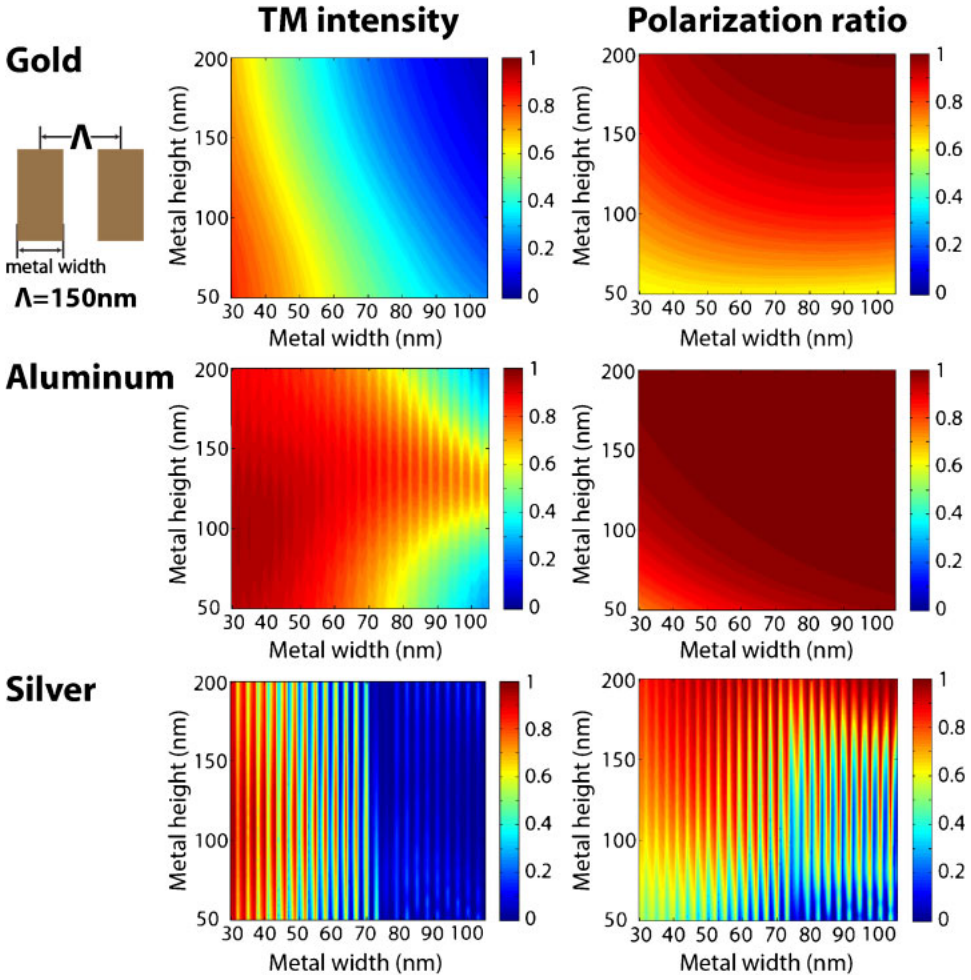

Fig. 2. (Color online) Simulated transmitted TM mode intensity ratio and polarization ratio as a function of the metal-stripe width and the metal-film thickness of different metals (Au, Al, and Ag).

the larger the metal width, the less light is transmitted through the WGP, and the higher the polarization ratio.

3. Experimental methods

The LEDs used in this study were grown by metal–organic vapor phase deposition on double-side polished *c*-plane sapphire. They were grown on *c*-plane sapphire with first a low temperature GaN buffer layer, followed by a 2-μm-thick unintentionally doped GaN layer. Next a 3-μm-thick Si-doped n-type GaN layer was grown followed by a five period GaInN/GaN multiple quantum well active region. After this, a p-type AlGaN electron blocking layer was grown followed by a p-type GaN capping layer. Mesa devices with 300 × 300 μm^2 chip area were fabricated under a standard LED fabrication process, followed by the depositions of reflecting n-type metal contacts (Ti/Al: 30/250 nm) and p-type metal contacts (NiZn/Ag: 5/200 nm).

After that, the Al WGP was fabricated on the backside of the fabricated LEDs. It is also important to note certain physical limitations for fabrication due to the resolution of electron-beam lithography as well as etch conditions. The period and the metal thickness chosen for fabrication were 150 and 190 nm, respectively, due to the high transmission percentage as well as polarization ratio. Although a period of 115 nm shows both good polarization ratio as well as transmitted power, it was not chosen because of the limitations with electron-beam lithography. Instead we chose 150 nm, as explained below. At first, an Al layer with a thickness of about 190 nm was deposited on the backside of the sapphire of the fabricated LEDs by using electron-beam evaporation. This was followed by electron-beam deposition of a layer of SiO_2 with a thickness of about 40 nm. Subsequently, a layer of the poly(methyl methacrylate) (PMMA) electroresist was spin-coated onto the SiO_2 layer. The SiO_2 was used as a hard mask to etch Al due to the poor etch resistivity of the electroresist, PMMA.[14,24] The PMMA was patterned by using electron-beam lithography to define a grating array within an area of 300 × 300 μm^2. The patterned resist has a period of 150 nm and a resist linewidth of about 75 nm, as shown in Fig. 4(a). The grating pattern was then replicated into the underlying SiO_2 layer through a fluorine-based inductively-coupled plasma reactive-ion etching (ICP-RIE) process. The SiO_2 layer was etched under 300 W ICP power with 15 sccm of CHF_3 at 10 mTorr to form the SiO_2 hard mask. The patterned SiO_2 has a period of 150 nm and a SiO_2 linewidth of about 90 nm, as shown in Fig. 4(b). Finally, the Al layer was etched through a chlorine-based ICP-RIE process by using the patterned SiO_2 as a hard mask. The Al layer was etched under 400 W ICP power with 30 sccm of BCl_3 and 10 sccm of Cl_2 at 5 mTorr. The Al nanowire gratings have a period of 150 nm and an Al linewidth of about 100 nm, as shown in Fig. 4(c).

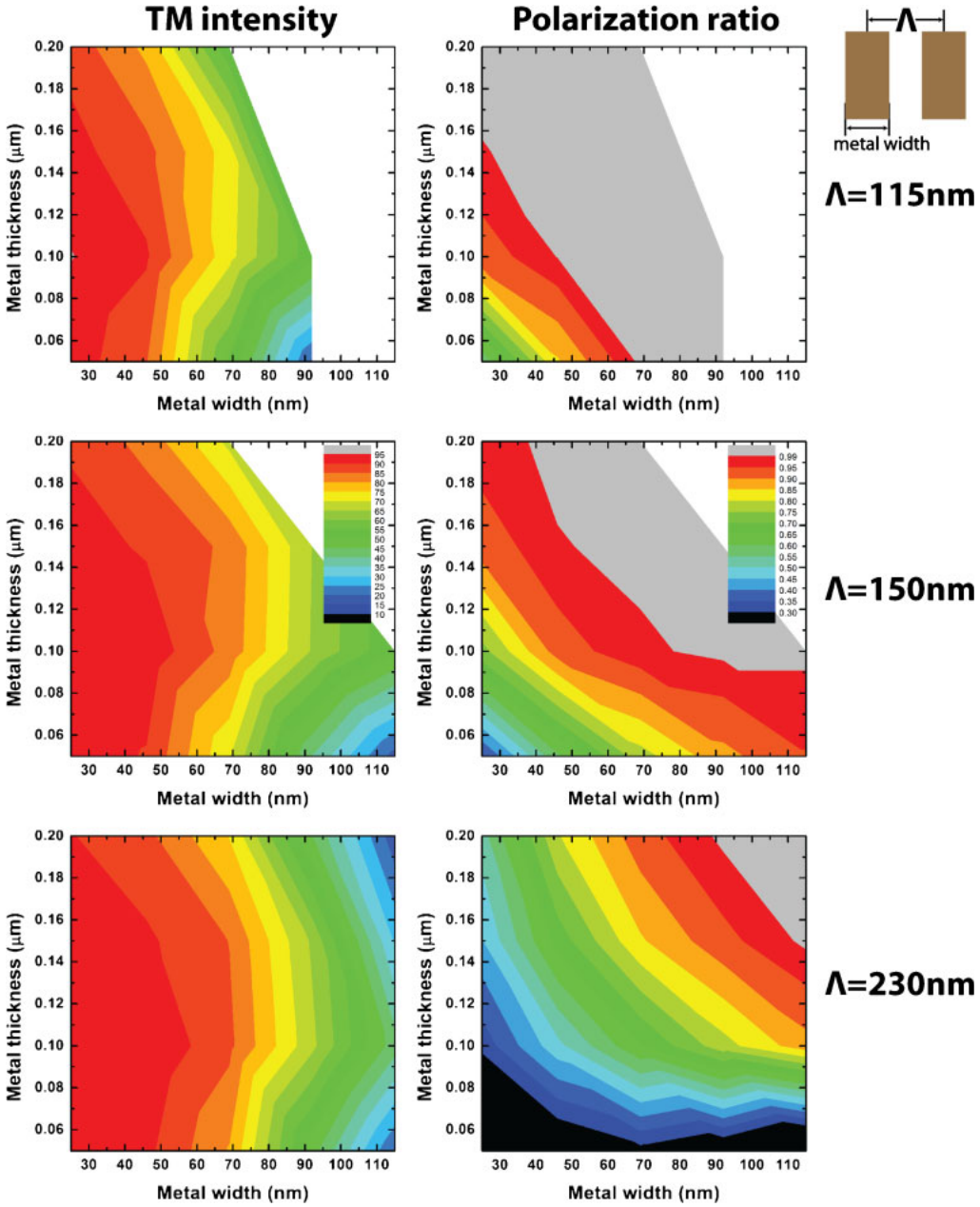

Fig. 3. (Color online) Simulated transmitted TM mode intensity ratio and polarization ratio, using an Al WGP, as a function of the metal-stripe width and the metal-film thickness.

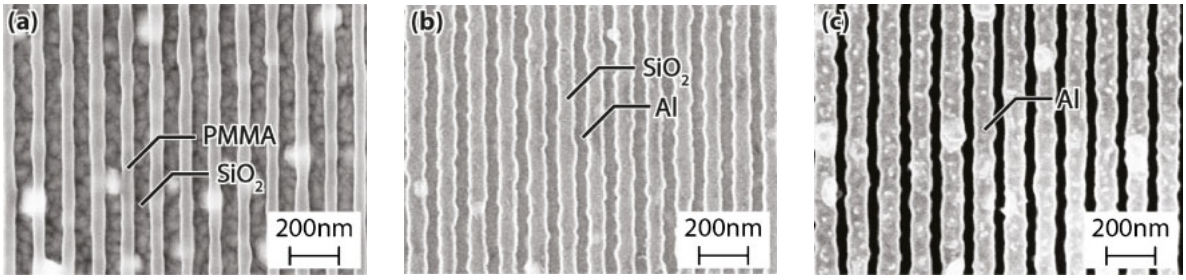

Fig. 4. (Color online) SEM images of (a) patterned PMMA on top of the SiO_2 layer, (b) patterned SiO_2 on top of the Al layer, and (c) Al WGP on top of the sapphire substrate.

4. Results and discussion

After fabrication, the polarization characteristics are investigated by utilizing a linear commercial polarizer in combination with a photodiode, as schematically illustrated in Fig. 5. A linear rotating polarizer is placed between the LED and the photodiode. This polarizer is considered an analyzing polarizer, as it is used to analyze the polarization character-

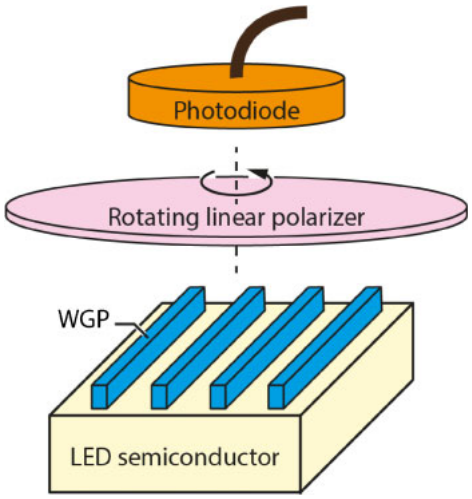

Fig. 5. (Color online) Schematic illustration of the measurement setup.

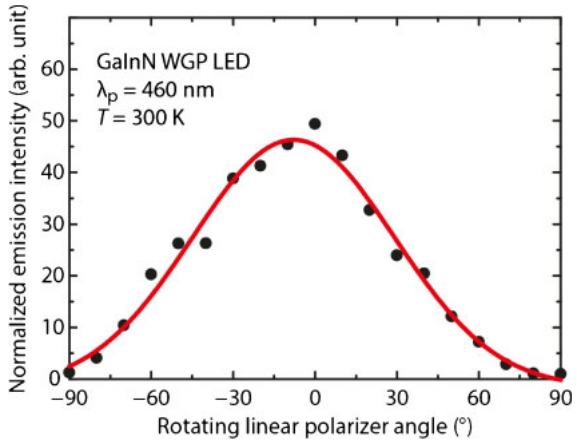

Fig. 6. (Color online) Measured electroluminescence intensity of the WGP LED as a function of the orientation angle of a rotating linear polarizer.

istics of the incident light. Before measuring the characteristic of WGP LEDs, we confirm that an LED without WGP shows completely unpolarized emission.

The WGP LEDs are probed and biased at several constant currents. At each current, the different polarizations of light are detected by rotating the analyzing polarizer in line with the designed direction of polarization. If the light read from the bottom is partially polarized, we should observe a difference in the light output as we rotate the analyzing polarizer with reference to the LED.

Figure 6 shows an angle dependent photocurrent. The measured intensity varies with the polarizer-rotating angle, revealing polarized light emission from the WGP LED. The maximum and minimum intensities indicate the relative magnitude of the TM mode light and TE mode light, respectively. The measured intensity of the TM mode light is about 50 times greater than the intensity of the TE mode light, corresponding to a polarization ratio of more than 90%. Note that our approach allows for an Al WGP with good uniformity and surface coverage since it is fabricated on the backside of the sapphire substrate, thus resulting in a high polarization ratio.

5. Conclusions

To conclude, simulation and fabrication of a nanometer scale WGP embedded on a GaInN based LED is demonstrated. A method to calculate the transmitted power intensities of TE and TM mode light is derived from Maxwell's equations. An optimized Al nanowire grating with a period of 150 nm is fabricated on the sapphire backside of a GaInN LED structure by electron-beam lithography and ICP-RIE. After fabrication of the polarized LED, a high polarization characteristic is observed experimentally. The polarized LED chip developed in this study may be combined with the reflector design in Ref. 20. A combination of these two technologies could yield a commercially viable product to be integrated into the growing LCD market.

Acknowledgments

The authors gratefully acknowledge support by the research funds of Chonbuk National University in 2014, and the Basic Research Laboratory Program (2011-0027956) of the National Research Foundation of Korea funded by Korea's Ministry of Education, Science and Technology.

1) J. Souk and S. Whangbo, Inf. Disp. **26** [12], 4 (2010).
2) P. Semenza, Inf. Disp. **27** [12], 14 (2011).
3) W. Lee, J. Park, V. Subramanian, and H. Takezoe, Opt. Mater. Express **4**, 1088 (2014).
4) Global TV 2010 — Markets, Trends Facts and Figures (IDATE, 2010).
5) P. Yeh and C. Gu, *Optics of Liquid Crystal Displays* (Wiley, New York, 2010) p. 4.
6) G. W. Gray and S. M. Kelly, J. Mater. Chem. **9**, 2037 (1999).
7) E. F. Schubert and J. K. Kim, Science **308**, 1274 (2005).
8) M. R. Krames, O. B. Shchekin, R. Mueller-Mach, G. O. Mueller, L. Zhou, G. Harbers, and M. G. Craford, J. Disp. Technol. **3**, 160 (2007).
9) S. Pimputkar, J. S. Speck, S. P. DenBaars, and S. Nakamura, Nat. Photonics **3**, 180 (2009).
10) R. Lu, S. Gauza, and S.-T. Wu, Mol. Cryst. Liq. Cryst. **488**, 246 (2008).
11) E. Hecht, *Optics* (Addison-Wesley, Reading, MA, 2001) 4th ed.
12) J. J. Wang, L. Chen, X. Liu, P. Sciortino, F. Liu, F. Walters, and X. Deng, Appl. Phys. Lett. **89**, 141105 (2006).
13) S. W. Ahn, K. D. Lee, J. S. Kim, S. H. Kim, J. D. Park, S. H. Lee, and P. W. Yoon, Nanotechnology **16**, 1874 (2005).
14) J. J. Wang, F. Walters, X. Liu, P. Sciortino, and X. Deng, Appl. Phys. Lett. **90**, 061104 (2007).
15) L. Zhang, J. H. Teng, S. J. Chua, and E. A. Fitzgerald, Appl. Phys. Lett. **95**, 261110 (2009).
16) P. P. Paskov, T. Paskova, P. O. Holtz, and B. Monemar, Phys. Status Solidi A **190**, 75 (2002).
17) N. F. Gardner, J. C. Kim, J. J. Wierer, Y. C. Shen, and M. R. Krames, Appl. Phys. Lett. **86**, 111101 (2005).
18) S. E. Brinkley, Y.-D. Lin, A. Chakraborty, N. Pfaff, D. Cohen, J. S. Speck, S. Nakamura, and S. P. DenBaars, Appl. Phys. Lett. **98**, 011110 (2011).
19) M. F. Schubert, S. Chhajed, J. K. Kim, E. F. Schubert, and J. Cho, Appl. Phys. Lett. **91**, 051117 (2007).
20) M. F. Schubert, S. Chhajed, J. K. Kim, E. F. Schubert, and J. Cho, Opt. Express **15**, 11213 (2007).
21) M. G. Moharam and T. K. Gaylord, J. Opt. Soc. Am. **71**, 811 (1981).
22) M. G. Moharam, E. B. Grann, D. A. Pommet, and T. K. Gaylord, J. Opt. Soc. Am. A **12**, 1068 (1995).
23) D. S. Meyaard, Master's thesis, Rensselaer Polytechnic Institute (2009).
24) M. Ma, D. S. Meyaard, Q. Shan, J. Cho, E. F. Schubert, G. B. Kim, M.-H. Kim, and C. Sone, Appl. Phys. Lett. **101**, 061103 (2012).